*34th EPS Conference on Plasma Phys. Warsaw, 2 - 6 July 2007 ECA Vol.**31F**, P-5.057 (2007)*

Geometric optics of lower hybrid waves in tokamak plasmas

C. Castaldo[1], A. Cardinali[1], A. Galli[2], G. Pasquariello[2], A. A. Tuccillo[1]

[1]*Euratom ENEA Assocation, Via Enrico Fermi 45, CP 65, I00044 Frascati, Italy*

[2]*University of Rome "La Sapienza", Rome, Italy*

Ray tracing of lower hybrid (LH) waves in steady state tokamak plasmas is commonly used to evaluate the quasilinear diffusion coefficients and calculate the LH power deposition and current drive profiles [1]-[3]. Accessibility condition imposes the use of slow-wave LH antennas, such that the near field is dominated by diffraction. However, for perfect axisimmetric configurations, the toroidal angle coordinate φ is ignorable, and ray tracing could be used in poloidal cross-section (with coordinates $\mathbf{x}=(R,Z)$). It then allows to evaluate the amplitude $\mathbf{E}_{n\varphi}(\mathbf{x})$ and the phase $S_{n\varphi}(\mathbf{x})$ of each Fourier component in the expansion:

$$E(\mathbf{x},\varphi,t) = \Sigma_{n\varphi}\, \mathbf{E}_{n\varphi}(\mathbf{x}) \exp\{i[S_{n\varphi}(\mathbf{x}) + n_{\varphi}\varphi - \omega t]\} \qquad (1)$$

Here we discuss the limits of the geometric optics of lower hybrid waves in the framework of a numerical analysis of the linear wave phase equation and quasilinear wave amplitude equation. Solov'ev analytical equilibrium is used, with poloidal flux:

$$\psi = \{(1/2)\,(bR_o^2 + R^2)Z^2\,[(a-1)/8]\,(R^2 - R_o^2)\}\,\psi_o \qquad (2)$$

Pure hydrogen plasma with linear plasma density profile $n_e(\psi)$ is assumed (the equilibrium also requires linear profiles vs ψ of both the plasma pressure P and the squared current flux function J^2); moreover it is assumed $T_e = 2T_i = 2P/(3n_e)$. Table I shows the main plasma and RF parameters of the scenario analyzed here, which represents a plasma discharge in the FTU tokamak [4], with additional (electron) heating.

B_o(T)	I_P(MA)	$n_o(m^{-3})$	$n_1(m^{-3})$	T_o(keV)	T_1(keV)	f (GHz)	P(MW)
7.0	0.7	$2.2\ 10^{20}$	$0.2\ 10^{20}$	5.0	0.2	8.0	1.0

Tab. I). Main plasma and RF parameters of the scenario considered. Values at the edge (subscript 1) are taken in the equatorial plane at R = 1.2 m. The magnetic axis is located in the equatorial plane at R = 0.96 m

A poloidally extended RF source is considered, which imposes at the plasma edge (low field side) a steady state electric field, with power spectrum vs the parallel wavenumber $n_{//}$ shown in Fig. 1. The linear tail in the interval $n_{//}$ = 2.1-4.0 represents the effect of spectral broadening due to nonlinear wave-plasma interactions occurring near the antenna mouth [5]-[7] .

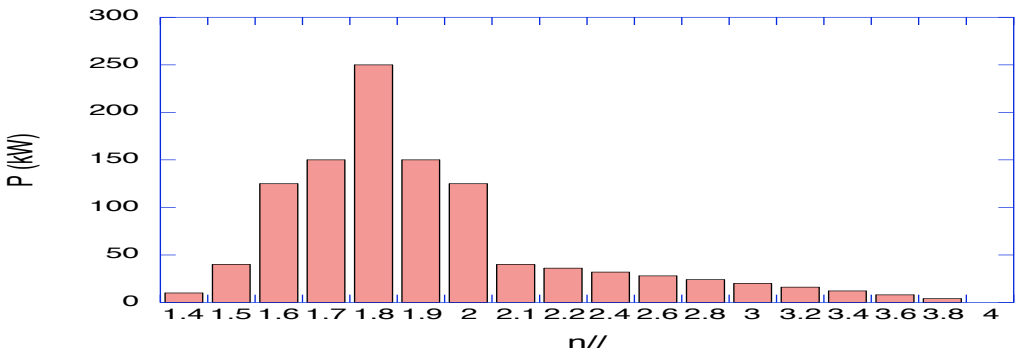

Fig.1) RF power spectrum vs n//.

Electrostatic, cold plasma approximation is used to evaluate the phase of each Fourier component by the ray tracing equations

$$d\mathbf{x}/dS = (\partial H/\partial \mathbf{k})/D_S \qquad (3)$$

$$d\mathbf{k}/dS = -(\partial H/\partial \mathbf{x})/D_S \qquad (4),$$

where $\mathbf{k} = \nabla S$ is the (local) wavevector projection in the poloidal cross section, H is the real part of the (local) longitudinal dielectric constant in the limit of cold plasma, $D_S = \mathbf{k}\bullet\partial H/\partial \mathbf{k}$, and, henceafter, the index n_φ has been omitted. The electric field polarisation is thus given by the direction of the full wavevector.

The quasilinear electric field amplitude equation along each ray is

$$d\,|\mathbf{E}|^2/\,dS = -(2\Gamma+\nabla\bullet\partial H/\partial \mathbf{k})/\,D_S \qquad (5),$$

where Γ is the imaginary part of the (local) longitudinal dielectric constant, for steady state electron distribution function. As a first step, the latter is calculated in the linear approximation, i.e. considering Maxwellian plasma, and $\Gamma = \Gamma_{lin}$. Once the linear electric field amplitude (using Γ_{lin}) and phase have been solved for each Fourier component, the quasilinear diffusion coefficient is evaluated, as a function of the parallel electron velocity and of the poloidal flux. A relativistic Fokker-Planck solver is then used to

evaluate the steady state electron distribution function and the corresponding (quasilinear) value $\Gamma = \Gamma_{qlin}$. The amplitude of the electric field is recalculated by (5). The results shown here reflect this stage of the solving method, although the iteration must be repeated, in principle, until the quasilinear diffusion coefficient converges.

Necessary conditions for the validity of the eikonal approximation are checked, namely (i) $|\mathbf{k}|L >> 2\pi$, where L is any characteristic length of variation of macroscopic plasma parameters (e.g. $L = 1/|\, n_e^{-1} \nabla n_e \,|$ for density) as well as of the the electric field amplitude or wavevector; (ii) $\kappa/|\mathbf{k}| << 1$, where κ is the ray (κ_{ray}) or wavefront ($\kappa_{wavefront}$) curvature; (iii) D_S not equal to 0.

In Fig. 2 the rays and the wavefronts obtained by numerical solution of (3) and (4) are shown for the fastest component $n_{//} = 1.4$, which is more critical for the eikonal theory validity . Edge reflection and central focusing lead to the failure of the eikonal approximation. The important result is that the assumed broadening of the LH spectrum occurring at the edge produces single-pass absorption (at $S \leq 800$ rad) due to quasilinear diffusion, thus preventing both focusing and edge reflection. Fig. 3-5 show that the eikonal approximation remains valid for the spectral component considered. As expected, it has been found that the slower components better satisfy the eikonal approximation requirements. The electric field amplitude, multiplyed by cos(S), for $n_{//} = 1.4$, is shown in Fig. 6: central focusing produces a divergence of the electric field amplitude if linear absorption is considerd (a); quasilinear damping prevent this effect (b).

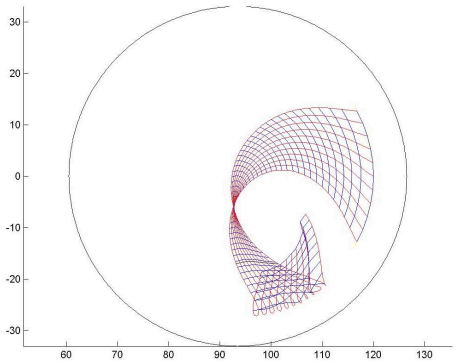

Fig.2) Ray tracing for $n_{//} = 1.4$. Abscissa is R (cm), ordiante is Z (cm). The phase difference of adjacent wavefronts is 40 rad.

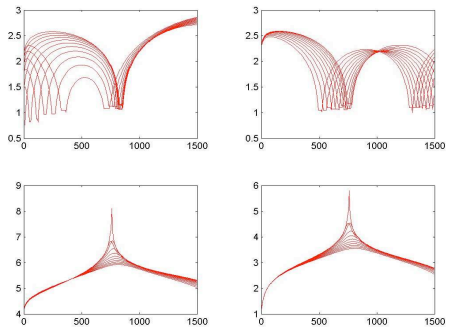

Fig. 3) Characteristic length of variation of B_R , B_z B_φ and n_e (clockwise from left up corner) in unit of $2\pi/|\mathbf{k}|$ vs S (rad). $n_{//} = 1.4$

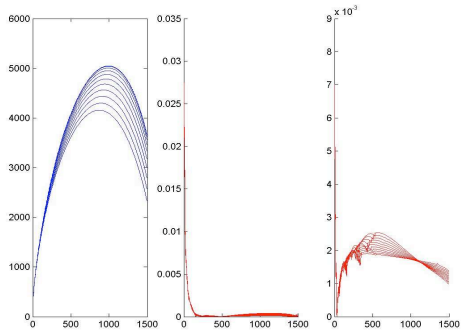

Fig.4) D_S , $\kappa_{ray}/|\mathbf{k}|$, $\kappa_{wavefront}/|\mathbf{k}|$ (from left) vs S (rad). $n_{//} = 1.4$

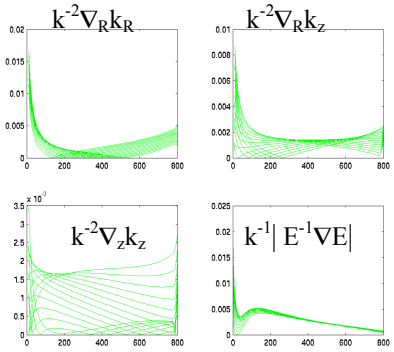

Fig. 5). Characteristic length of variation of **k** and $|\mathbf{E}|$ in unit of $1/|\mathbf{k}|$ vs S (rad). $n_{//} = 1.4$

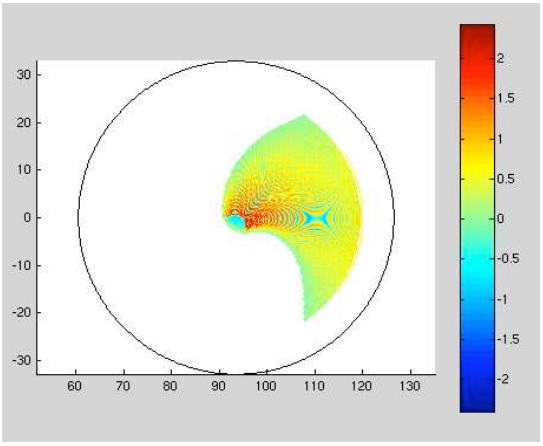

Fig. 6a) Electric field (stV/cm) amplitude x cos(S) of the component $n_{//} = 1.4$ in poloidal cross section. Linear theory is applied.

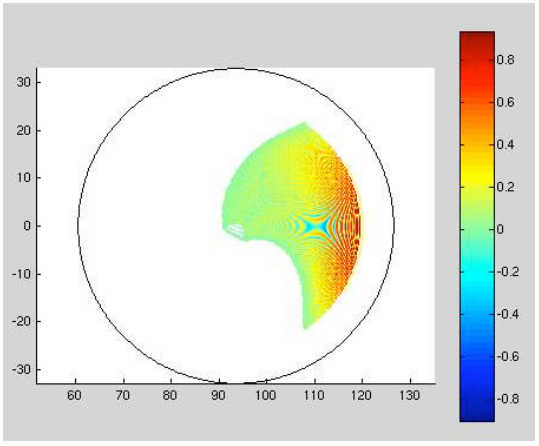

Fig. 6b) Quasilinear electric field (stV/cm) amplitude x cos(S) of the component $n_{//} = 1.4$ in poloidal cross section.

The authors are grateful to R. Cesario for valuable comments

References:

[1] Ira B. Bernstein, and L. Friedland, in Handbook of Plasma Physics, ed. By A. Galeev and R.N. Sudan (North Holland, Amsterdam, 1984), Vol. 1, p. 367
[2] N. Fish, Rev. Modern Phys. **59**, 175 (1987)
[3] A. Cardinali, Recent Res. Devel. Plasmas, **1**, 185 (2000)
[4] Fusion Science and Technology, **45** (2004) Special Issue on Frascati Tokamak Upgrade (FTU)
[5] R. Cesario, et al., Phys. Rev. Lett., **92** (2004) 17502
[6] R. Cesario, et al., Nucl. Fusion **46** (2006) 462
[7] C. Castaldo, et al., Physics Letters A **230**, 336 (1997)